Fluxonic Properties of Vortices in a Washboard Pinning Potential Fabricated by Focused Particle Beam Techniques

O.V. Dobrovolskiy[a,*], M. Huth[a] and V.A. Shklovskij[b,c]

[a]Physikalisches Institut, Goethe-University, 60438 Frankfurt am Main, Germany

[b]Institute of Theoretical Physics, NSC-KIPT, 61108 Kharkiv, Ukraine

[c]Physical Department, Kharkiv National University, 61077 Kharkiv, Ukraine

A challenging aspect of the usage of patterned nanostructures relates to the development of superconducting devices operating with the Abrikosov vortices in some pinning potential. To provide such a potential we have used thin epitaxial films of Nb with washboard-like nanostructures in the form of grooves or Co stripes. The nanostructures were prepared by focused ion beam milling or focused electron beam induced deposition, respectively. The results of transport measurements affirm the existence of two fluxonic effects, the guided vortex motion and the vortex ratchet effect, both invoked by the nanostructuring. In particular, the effects represent the basis for the development of advanced fluxonic devices using a directional or orientational control of the net vortex motion in Nb films nanostructured by focused particle beam techniques.

PACS: 74.25.F−, 74.25.Wx, 74.25.Sv

1. Introduction

It is well known that a type-II thin-film superconductor, while exposed to an external magnetic field whose magnitude is between the lower and upper critical field, is penetrated by a flux-line array of the Abrikosov vortices. In a perpendicular magnetic field, the vortex array moves with average velocity $\boldsymbol{v}$ under the action of the Lorentz force $\boldsymbol{F}_L$ essentially perpendicular to applied dc or ac currents. Due to the nonzero viscosity experienced by the vortices when moving through the superconductor, a faster vortex motion corresponds to a larger dissipation. To reduce this, the vortex motion can be impeded or deflected by the introduction of vortex pinning sites into the superconductor which act as potential wells for the potential energy of the vortices [1]. As possible sources of such potential wells can serve, e.g., local reductions of the thickness of the superconductor perpendicular to the magnetic field [2], ferromagnetic decorations on top of the superconductor [3], pre-patterned [4] or facetted [5] substrates. As a result, the nonlinear two-dimensional vortex dynamics becomes strongly anisotropic, as $\boldsymbol{v}$ and $\boldsymbol{F}_L$ in general are not collinear. The guided vortex motion, or the *guiding effect* represents the most important manifestation of such an anisotropy, as the vortices tend to move along the pinning potential "channels" rather than to overcome their potential barriers.

An intriguing effect appears when the pinning potential landscape (PPL) is asymmetric. In this case the reflection symmetry of the pinning force in the direction perpendicular to the PPL channels is also broken and

thus, the critical currents corresponding to the strong- and weak-slope PPL directions are not equal. As a result, while subjected to an ac current drive of zero mean, whose magnitude is between these critical current densities, a net rectified motion of the vortices occurs. This is known as a rocking *ratchet effect* and has been widely used for studying the basics of the mixed-state physics, e.g. by removing the vortices from conventional superconductors [6], as well as to verify ideas of a number of nanoscale systems, both solid state and biological [7].

Within the last decade the idea to manipulate the Abrikosov vortices, also called fluxons, has attracted considerable attention [8]. This is nowadays known as fluxonics, similarly with the control of electrons in electronics. Fluxonics mainly relies upon the guiding and ratchet effects in the vortex dynamics, as described above, and implies the usage of nanostructured PPL's for the tailoring of vortex-confining potentials. In particular, by varying the external magnetic field value B, one can alter the vortex density and thus move between regimes of independent vortices and collective phenomena with strongly interacting vortices. It should be noted that so far only fluxonics devices with linearly extended pinning sites of a washboard type have a most full and exact theoretical description [9] of their magnetoresistive and microwave properties. This description is valid at least at small magnetic fields. Evidently, to investigate both, the guiding and ratchet effects in superconductors with carefully designed potential landscapes on the nm scale, advanced nanofabrication tools must be applied.

Recently the explosive development of the nanotechnology has led to the appearance of advanced nanofabrication tools, such as focused particle beam processing techniques [10], which allow one to alter the material in conformity with a predefined pattern in the nanometer

* corresponding author; e-mail:
Dobrovolskiy@Physik.uni-frankfurt.de

range. Such maskless direct writing techniques represent an alternative for conventional lithographic techniques with advantages of a tunable pinning intensity by varying the height (depth) of the structure, the high periodicity of the profile, and the availability of non-patterned (as-grown) films for reference purposes.

In the present work we employed two complementary direct nanofabrication tools, either focused electron beam induced deposition (FEBID) to furnish superconducting Nb thin films with an array of Co stripes or focused ion beam (FIB) milling to create uniaxial asymmetric grooves, as illustrated in Fig. 1. Details concerning the nanostructuring process and beam parameters can be found in Ref. [11]. Below we show selected results of transport measurements which demonstrate the guiding and ratchet effects, as main prospects for the nanodevices' development.
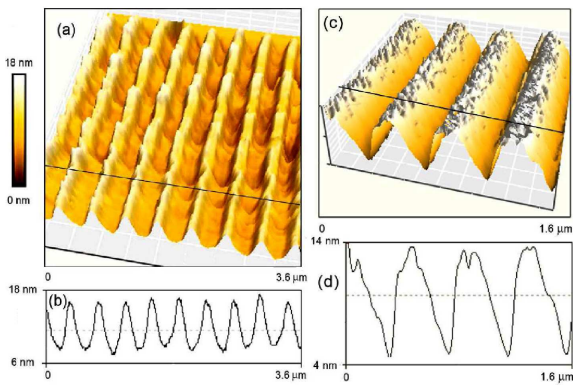

Fig. 1. AFM images of the film surface with nanofabricated pinning landscapes. (a) A uniaxial profile fabricated by FEBID of an array of Co stripes (sample I). (c) A ratchet landscape with grooves milled by FIB (sample II). (b) and (d) Line scans of the nanoprofiles, as indicated.

2. Results and discussion

Before entering the discussion of the obtained results, we briefly address the experimental geometry. An 8-contact bridge in sample I and a 4-contact bridge in sample II, both with an area of $48 \times 48\ \mu m^2$, have been defined by photolithography and Ar ion-beam etching techniques. Uniaxial symmetric (Fig. 1a) and ratchet (Fig. 1b) pinning landscapes have been prepared within the inner parts of the bridges, respectively. A dc transport current density of $10\ kA/cm^2$ and a perpendicular magnetic field of 10 mT have been used. Sample I was used to check the directional control of the vortex motion, whereas sample II was used to verify the orientational one. Both samples allow one to investigate the two basic geometries, transverse and longitudinal.

In the transverse geometry vortices move across the PPL channels, while the transport current is applied along the PPL channels, i.e., $\alpha = 0°$ (see, e.g., inset in Fig. 2b). In the longitudinal geometry vortices move along the PPL channels, whereas the current flows across them, i.e., $\alpha = 90°$. In addition, sample I enables one to rotate the current $I = (I_x^2 + I_y^2)^{1/2}$ in its plane and to study the total magnetoresistive response $R = (R_x^2 + R_y^2)$, with $I_x = I \sin\alpha$, $I_y = I \cos\alpha$, where R_x and R_y are measured as shown in the inset of Fig. 2a.
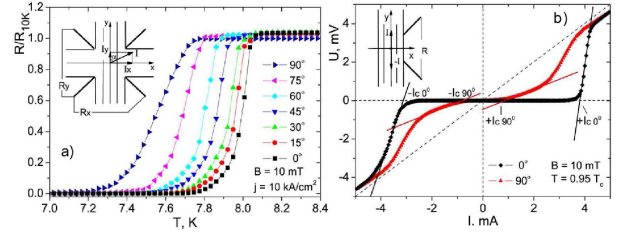

Fig. 2. (a) Temperature dependences of the total resistance of sample I for a set of transport current orientations α with respect to the stripes guiding direction, as indicated. R_{10K} is the normal-state resistance at $T = 10$ K. (b) Current–voltage characteristics of sample II at $T = 0.95T_c$. The vertical and horizontal dashed lines are shown to guide the eye. The diagonal dashed line corresponds to Ohm's law. Thin solid lines are plotted to illustrate estimations for the critical current densities. Insets: the 8- and 4-contact bridges with PPL channels parallel to the y-axis illustrate the geometry of the measurements for both samples.

Selected samples parameters are summarized in Table. In Fig. 2a the temperature dependence of the total resistance $R(T)$ of sample I is shown for different transport current orientations α with respect to the stripes guiding direction. As it is seen from Fig. 2a, the total resistance of sample I is substantially anisotropic and strongly depends on the angle α. In the limiting case of the longitudinal geometry, $\alpha = 90°$, vortices being influenced only by the "background" isotropic pinning sites, which are always present due to impurities, move along the fabricated PPL channels. This leads to a pronounced dissipation, thus a pronounced nonzero "tail" is observed at lower temperatures. In the opposite limiting case of the transverse geometry the vortices are pinned to the PPL sites and the superconducting state is preserved up to higher temperature, when the vortices finally are thermally excited from the PPL minima. The resistive transition in this case is most sharp. For the intermediate angles $\alpha = 15°, 30°, 45°, 60°, 75°$ with increasing temperature, the vortex movement changes consequently its character from a thermally activated motion to that of viscous flux flow with respect to both, isotropic and anisotropic, pinning potentials. A difference less than 4% in the normal-state resistivity values for the different α can be attributed to a small violation of the etched bridge from the regular square form.

TABLE

Samples parameters.

	Thickness d [nm]	Inner bridge	Type of pattern	Process	$T_c(B = 0)$ [K]	$\Delta T_c(B = 0)$ [K]	RRR
sample I	52	8-contact	symmetric	FEBID	8.05	< 0.1	12
sample II	54	4-contact	ratchet	FIB	8.15	< 0.1	14

The current–voltage characteristics (CVCs) of sample II are shown in Fig. 2b at $T = 0.95T_c$. Considering firstly the longitudinal geometry, several features of the CVC should be noted. The CVC is an odd function with regard to the change $I \to -I$ or $B \to B$ and demonstrates a strongly nonlinear shape. The reason of such a non-ohmic behavior is the isotropic pinning, which is relatively weak due to its "background nature". By crossing the current axis by a tangent line to the CVC traced close to the point of its rapid increase, one can determine the critical current density j_c for both the current directions (see Fig. 2b). Taking into account the geometrical dimensions of sample II one obtains $|+j_{c\,90°}| = |-j_{c\,90°}| \approx 35$ kA/cm^2. This value is substantially smaller than typical values resulting in the next case of the transverse geometry where the CVC is asymmetric, i.e., is not an odd function with regard to the change $I \to -I$ or $B \to -B$. In this case the left- and right-hand branches of the CVC have different slopes and the nonlinear transitions occur at nonequal currents. Let us consider the right-hand branch of the CVC and the transport current flowing along the grooves such that the vortices move across the PPL channels in the strong-slope direction. This branch of the CVC demonstrates a sharp step-like behavior with $|+j_{c\,0°}| \approx 150$ kA/cm^2. The polarity change of the transport current invokes the vortex motion in the weak-slope direction of the PPL. There, the nonlinear transition occurs at $|+j_{c\,0°}| \approx 115$ kA/cm^2 which is still much stronger than in the transversal geometry. The difference by a factor of about 1:3 in the crossover currents in the right and left branches of the CVC in the transversal geometry represents a clear manifestation of the ratchet behavior [12]. In the frame of that work [12] this ratio can be brought into correlation with the asymmetry of the nano-fabricated PPL.

Concluding, a clear difference in the crossover currents for the vortex movement along and across the PPL channels has been observed in a Nb film furnished by a Co nanostripe array. Under current reversal, the sample with asymmetric PPL invoked by FIB milled grooves demonstrates distinct crossover current densities depending on the strong- or weak-slope directions of the PPL impeding the vortex motion. The discussed crossover current differences represent the basis for the development of advanced superconducting devices on the basis of two particular fluxonic effects, the guiding vortex mo-

tion and the ratchet effect, which allow one a directional and orientational degree of control of the net vortex motion, respectively.

Acknowledgments

References

[1] G. Blatter, M.V. Feigelman, V.B. Geshkenbein, A.I. Larkin, V.M. Vinokur, *Rev. Mod. Phys.* **66**, 1125 (1994).

[2] D.D. Morrison, R.M. Rose, *Phys. Rev. Lett.* **25**, 356 (1970).

[3] Y. Yuzhelevski, G. Jung, *Physica C* **314**, 163 (1999).

[4] J.I. Martin, Y. Jaccard, A. Hoffmann, J. Nogues, J.M. George, J.L. Vicent, I.K. Schuller, *J. Appl. Phys.* **84**, 411 (1998).

[5] O.K. Soroka, V.A. Shklovskij, M. Huth, *Phys. Rev. B* **76**, 014504 (2007).

[6] C.S. Lee, B. Janko, I. Dereny, A.L. Barabasi, *Nature* **400**, 337 (1999).

[7] B.L.T. Plourde, *IEEE Trans. Appl. Supercond.* **19**, 3698 (2009).

[8] A.V. Silhanek, J. Van de Vondel, V.V. Moshchalkov, in: *Nanoscience and Engineering in Superconductivity*, Eds. V. Moshchalkov, R. Wördenweber, W. Lang, Springer-Verlag, Berlin 2010, p. 1.

[9] V.A. Shklovskij, A.A. Soroka, A.K. Soroka, *J. Exp. Theor. Phys.* **89**, 1138 (1999); V.A. Shklovskij, *Phys. Rev. B* **65**, 092508 (2002); V.A. Shklovskij, O.V. Dobrovolskiy, *Phys. Rev. B* **74**, 104511 (2006); **78**, 104526 (2008); **84**, 054515 (2011).

[10] I. Utke, P. Hoffmann, J. Melngailis, *J. Vac. Sci. Technol. B* **26**, 1197 (2008).

[11] O.V. Dobrovolskiy, M. Huth, V.A. Shklovskij, *J. Supercond. Nov. Magnet.* **24**, 375 (2011).

[12] V.A. Shklovskij, V.V. Sosedkin, *Phys. Rev. B* **80**, 214526 (2009).